Chinese Chemical Letters 35 (2024) 109864

Contents lists available at ScienceDirect

Chinese Chemical Letters

journal homepage: www.elsevier.com/locate/cclet

Enhanced circularly polarized luminescence emission promoted by achiral dichroic oligomers of F8BT in cholesteric liquid crystal

Yang Li[a,c,*], Yihan Chen[a,b], Jiaxin Luo[a], Qihuan Li[a], Yiwu Quan[b], Yixiang Cheng[a,*]

[a] State Key Laboratory of Analytical Chemistry for Life Science, School of Chemistry and Chemical Engineering, Nanjing University, Nanjing 210023, China
[b] Key Laboratory of High Performance Polymer Material and Technology of Ministry of Education, School of Chemistry and Chemical Engineering, Nanjing University, Nanjing 210023, China
[c] Wenzhou Institute, University of Chinese Academy of Sciences, Wenzhou 325001, China

ARTICLE INFO

Article history:
Received 20 February 2024
Revised 2 April 2024
Accepted 6 April 2024
Available online 8 April 2024

Keywords:
Circularly polarized luminescence
Cholesteric liquid crystal
F8BT
Dichroism
Compatibility

ABSTRACT

In the exploration of circularly polarized luminescence (CPL) materials, doping cholesteric liquid crystals (CLCs) with achiral dyes is a common strategy. Conjugated polymers are favored as achiral dyes for their superior luminescent properties. In this study, a series of oligomers (M1-M3) and the conjugated polymer F8BT were synthesized to systematically assess the impact of the length of the conjugated backbone on CPL signals of CLCs doped with conjugated polymers. As the length rose from M1 to M3, CPL intensity concurrently increased ($|g_{lum}|$ increased from 0.35 to 0.84), attributable to enhanced dichroism (order parameter, S_F increased from 0.20 to 0.56). In contrast, F8BT polymer resulted in diminished CPL intensity ($|g_{lum}| = 0.64$) due to the reduced compatibility. Achieving a balance between dichroism and compatibility is crucial for optimizing CPL in conjugated polymer-doped CLCs. The guiding principle established here may have broad applicability in other CPL assemblies, offering a strategic avenue to engineer high-performance CPL materials with conjugated polymer.

Cholesteric liquid crystals (CLCs) are renowned for their ordered, chiral structure with long-range molecular organization, positioning them as valuable in various domains, including optoelectronics, data encryption and biotechnology [1–10]. Recent advancements have shown that CLCs can significantly enhance the circularly polarized luminescence (CPL) of achiral dyes through chiral co-assembly approach [11–14]. This enhancement is attributed to the helical superstructure and the intermolecular exciton coupling of achiral dyes [15,16]. Utilizing CLC platforms, a growing number of CPL-active materials with high dissymmetry factors (g_{lum}) and tunable fluorescence has been developed [17–21]. Since 2019, our team has been leading the creation of potent CPL materials, achieving $|g_{lum}|$ values up to 1.42 by integrating achiral dyes into the CLC framework [22–24]. Conjugated polymers, known for their semiconducting and luminescent properties, are considered excellent candidates for advanced optoelectronic applications [25–28]. We have explored these polymers as achiral dyes within emissive CLC systems for CPL production. For instance, in 2020, we introduced an achiral conjugated fluorescent polymer into CLCs, which showed robust CPL with a g_{lum} value of 1.12 [29]. More recently, we utilized the red luminescent conjugated polymer DTBTF8 to establish a co-assembled CLC system that produced exceptionally strong CPL signals ($g_{lum} = 0.7/-0.67$) [30].

The excellent CPL performance of CLCs doping with conjugated polymer can be attribute to the high order degree originating from their high length-diameter ratio [31]. Research indicates that CPL characteristics in emissive CLCs are influenced not only by the helical superstructure but also by the dichroism of the achiral dyes (quantified by order parameter S_F) [32]. Scholes and colleagues reported that conjugated polymers can assume a highly stretched conformation in a liquid crystal matrix, with their high aspect ratio and rigidity offering significant dichroic effects, making them ideal for boosting CPL in CLCs [33]. However, the study of CLC materials doped with conjugated polymers is rare, possibly due to the polymers' limited matrix compatibility [34]. Balancing the polymers' dichroism with their compatibility in the CLC matrix is a challenge yet to be overcome.

Oligomers with uniform structure and monodisperse molecular weight are ideal candidates for fundamental studies [35,36]. We synthesized a sequence of oligomers, M1-M3, along with the conjugated polymer poly(9,9-dioctylfluorene-*alt*-benzothiadiazole) (F8BT) (Scheme 1a), aiming to explore how the length of the conjugated backbone affects dichroism and material compatibility.

* Corresponding authors.
E-mail addresses: liyangchem@foxmail.com (Y. Li), yxcheng@nju.edu.cn (Y. Cheng).

https://doi.org/10.1016/j.cclet.2024.109864
1001-8417/

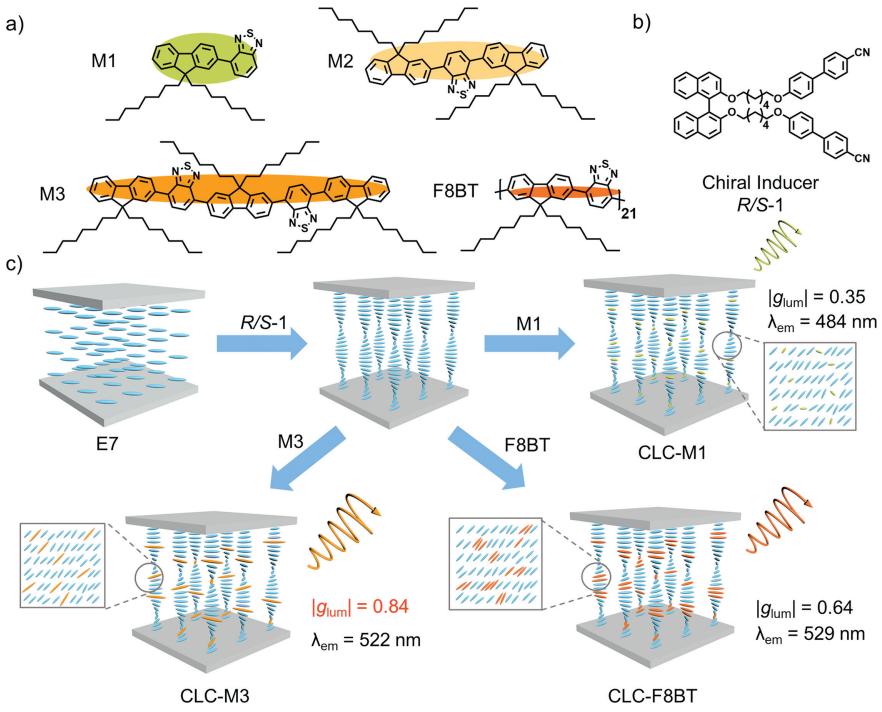

Scheme 1. (a) molecular structures of oligomers M1-M3 and F8BT. (b) Molecular structure of chiral inducer *R*/*S*-1. (c) Schematic illustrations of the molecular alignment of M1, M3 and F8BT in CLCs.

These achiral dyes, ranging from M1 to M3 and including F8BT, were incorporated into a CLC matrix (formulated by blending a chiral inducer (*R*/*S*-1) with the nematic liquid crystal E7 as shown in Schemes 1b and c) to craft CPL-active CLCs [37]. A marked increase in dichroism was noted, escalating from 0.20 to 0.56, as the length climbed from M1 to M3. This progression mirrored in the CPL intensities for M1, M2, and M3-doped CLCs, with $|g_{lum}|$ values of 0.35, 0.71, and 0.84, respectively. It was evident that as the repeating units extended, the enhancement in the S_F and the g_{lum} began to plateau. However, when the length of the conjugated backbone was further increased to the level of the conjugated polymer F8BT, the compatibility with the host structure became a pivotal factor influencing the CPL efficiency. This was due to F8BT's propensity to form misaligned aggregates, which led to a decrease in S_F (0.53) and CPL intensity ($|g_{lum}| = 0.64$). Among the tested compounds, the M3-doped CLCs demonstrated superior dichroism ($S_F = 0.56$) and $|g_{lum}|$ value (0.84), showcasing an optimal balance between dichroism and compatibility. Our findings point to a promising method for developing high-performance CPL materials with achiral conjugated polymers.

The synthesis and characterization of oligomers M1-M3 and F8BT were detailed in Supporting Information. The molecular weight of F8BT was determined by gel permeation chromatography ($M_n = 11{,}099$ g/mol, $M_w = 18{,}707$ g/mol, PDI = 1.69). In our initial analysis, we examined the photophysical properties of oligomers M1-M3 and the polymer F8BT in tetrahydrofuran (THF) at a uniform concentration of 10^{-5} mol/L. As illustrated in Fig. 1a, these substances showed distinct absorption peaks at wavelengths of 376, 416, 430, and 453 nm. These peaks are indicative of the intramolecular charge transfer (ICT) from the fluorene units to the benzothiadiazole units [35]. Notably, there was a consistent pattern of redshift across the spectrum, which we attribute to an extension in the conjugated chains coupled with a narrowing of the energy gap between the highest occupied molecular orbital (HOMO) and lowest unoccupied molecular orbital (LUMO) (Fig. S1 in Supporting information) [38]. Fig. 1b displays the normalized emission spectra, with the fluorescence (FL) of M1 peaking at 484 nm,

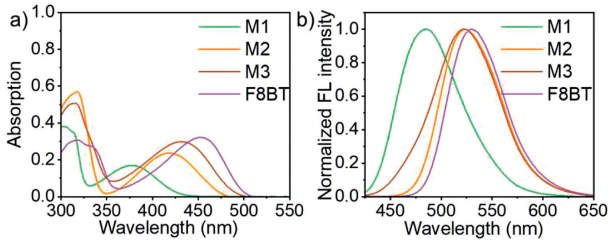

Fig. 1. The (a) absorption and (b) normalized emission spectra of achiral dyes M1-M3 and F8BT in THF solution (1×10^{-5} mol/L).

while the fluorescence peaks for M2, M3, and F8BT were all observed near 525 nm. Further experiments altering the solvent conditions indicated a significant bathochromic shift in the photoluminescence of M1-moving from 454 nm in non-polar hexane to 504 nm in polar acetonitrile (Fig. S2a in Supporting information). A similar trend of bathochromic shifts was consistently observed for the other dyes as well (Fig. S2 in Supporting information), affirming the influence of ICT on their photoluminescence behavior [32]. From these results, we may infer that the fluorescence transition dipole moment (TDM) vectors are aligned with the conjugated fluorene-benzothiadiazole structure of the dyes.

Due to variations in the conjugation length, the ratio of length to diameter for the oligomers and F8BT progressively increased, as shown in Scheme 1a. Luminescent nematic liquid crystals, designated as NLCs-M1, M2, M3, and F8BT, were prepared by dispersing the achiral oligomers and F8BT into the ambient temperature LC host E7 at a 1.0 wt% concentration [31]. We then conducted S_F analysis using polarized fluorescence spectroscopy as Eq. S1 (Supporting information). The findings, as presented in Fig. 2, indicate that for all dyes, the fluorescence intensity parallel to the alignment of the liquid crystal cells ($F_{\parallel}$) was higher than that in the perpendicular direction ($F_{\perp}$), indicating positive dichroism [39]. Among them, M3 exhibited the highest S_F, reaching 0.56, while M1 showed a lower value of 0.20, which may be attributable to the

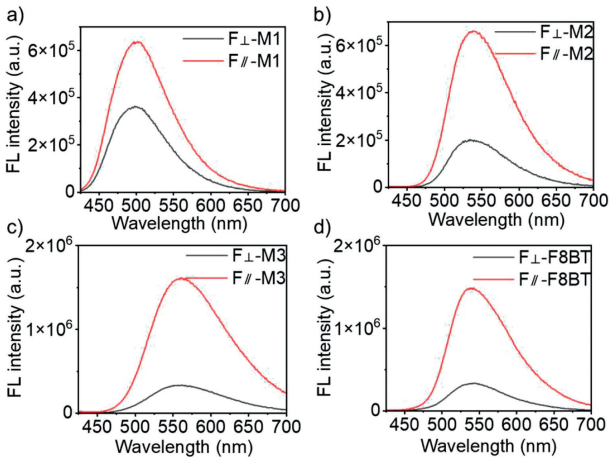

Fig. 2. Polarized fluorescence spectra of achiral dyes (a) M1, (b) M2, (c) M3, and (d) F8BT in the parallelly aligned LC cells.

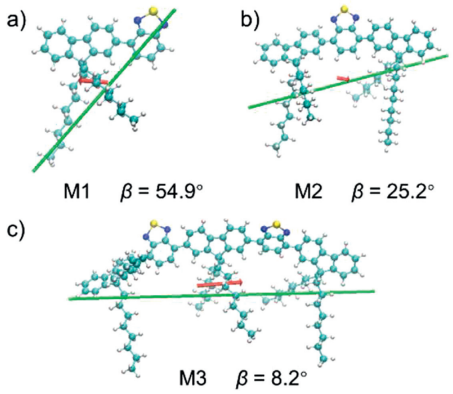

Fig. 3. The MOI axis (green rod) and TDM vectors (red arrow) of oligomers (a) M1, (b) M2, (c) M3 by DFT calculations.

increasing ratio of length to diameter from M1 to M3 [40]. This ratio of length to diameter and the stretched configuration within the CLCs seem to facilitate the ordered alignment of the achiral dyes [41]. Conversely, the longer conjugation of F8BT reduced its orientation order ($S_F = 0.53$) which may be due to the lower compatibility with the E7 host, as depicted in Scheme 1c.

To elucidate the link between the order parameter (S_F) and the molecular architecture of the achiral oligomers, we employed density functional theory (DFT) calculations. These calculations focused on the minimum moment of inertia (MOI) axis and the TDM vectors, utilizing the B3LYP/6–31 G level of theory within the Gaussian 09 software suite [42]. Fig. 3 shows a discernible shift in the MOI axis (green rod): it pivots from an angled orientation relative to the conjugated main chain to a more parallel alignment as the number of repeating units grows (from M1 to M3). Consequently, the angle θ, as defined in Eq. S2 (Supporting information), is expected to widen due to the increasing competitive interactions between the dyes' conjugated main chains and their alkyl side chains within the E7 host [43]. Additionally, the fluorescence TDM vectors were suggested to be intramolecular charge transfer (ICT) from the fluorene donor segments to the benzothiadiazole acceptor units (Fig. 1). As indicated in Fig. 3, the β angles between the MOI and TDM vectors for the oligomers M1-M3 series vary, decreasing from 54.9° to 8.2° with an increase in conjugation length. According to Eq. S2, M1's larger β angle (54.9°) corresponded with a lower S_F value (0.20), whereas M3's MOI closely paralleled the TDM, resulting in a smaller β angle (8.2°) and a higher S_F value (0.56). Therefore, increasing oligomer length is an efficient way to enhance the S_F value by molecular extension in CLCs matrix.

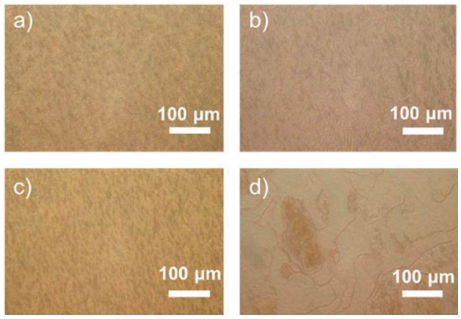

Fig. 4. POM images of (a) CLC-M1, (b) CLC-M2, (c) CLC-M3 and (d) CLC-F8BT in flat LC cells.

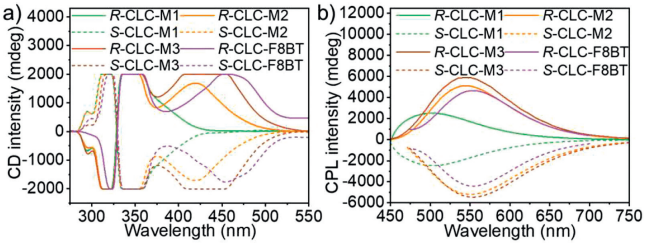

Fig. 5. (a) CD and (b) CPL spectra of *R*/*S*-CLC-M1, *R*/*S*-CLC-M2, *R*/*S*-CLC-M3, and *R*/*S*-CLC-F8BT.

Oligomers M1-M3 and F8BT were then added to the CLC host (prepared by doping chiral inducer *R*/*S*-1 into E7 host) to form the corresponding emissive CLCs. The chiral inducer and achiral dye concentrations were optimized to be 1.0 wt% and 1.0 wt% by measuring the CPL signals (Fig. S3 in Supporting information). CLCs-M1, CLCs-M2, CLCs-M3, and CLCs-F8BT were prepared by doping 1 wt% of *R*/*S*-1 and 1 wt% of achiral dye (oligomers M1-M3 and F8BT) into E7 for polarizing optical micrograph (POM) and photophysical measurement of the CLCs. As is evident from Fig. 4 and Fig. S4 (Supporting information), the resulting CLCs could spontaneously align as typical and ordered fingerprint textures. This can be due to the formation of regular helically twisted structures [20]. The aggregate of F8BT could be observed in the CLC and indicating the compatibility problem [44]. This may be the key reason for lower dichroism character. By lowering the concentration of F8BT in CLCs to 0.25 and 0.1 wt%, the aggregate remains existence (Fig. S5 in Supporting information) indicating the aggregate phenomenon (low compatibility) was mainly due to the high conjugation length of F8BT. Notably, the helical pitches of CLCs were calculated using the planar Grandjean-Cano lines on the POM images (Fig. S6 in Supporting information) [45,46]. Only a small change was observed in the helical pitches of the CLCs. We can propose that achiral oligomers and F8BT had a very weak influence on the texture arrangement of CLCs.

We further examined the chiroptical characteristics of four CLCs by measuring their circular dichroism (CD) spectra. As depicted in Fig. 5a, each CLC displayed distinct CD bands that mirrored each other between 295 nm and 360 nm, indicative of the characteristic absorption stemming from the chiral dopant inducer co-assembling with the E7 host [47]. Notably, the CLCs-M1-M3 and CLCs-F8BT revealed new, mirrored Cotton effects in the longer wavelength span of 375-500 nm, aligning perfectly with the absorption spectra of the achiral oligomers M1-M3 and F8BT shown in Fig. 1a. This result suggests successful chiral induction from the

chiral inducer to the achiral oligomers M1-M3 and F8BT within the E7 host, facilitated by a supramolecular co-assembly process that arranges the achiral dyes into a helical structure (Scheme 1c) [48,49]. Among these, M3-which exhibited the highest dichroism (S_F)-demonstrated stronger CD signals. This implies a more orderly parallel alignment with the E7 host molecules, resulting in a more structured helical configuration within the CLC patterns. In contrast, M1, which had a lower S_F, showed a less distinct CD peak and tended towards a less ordered state, suggesting a reduced efficiency in chiral transfer and induction compared to M3 within the same CLC host due to the lower length-diameter ratio. F8BT's CD signals not only showed a noticeable redshift but were also slightly less intense than those of M3, a trend that correlated with the S_F values (Fig. 2). This could be attributed to compatibility issues where the aggregates formed within the CLCs (Fig. 4) diminish the degree of order and, consequently, the CD signal strength [50]. Thus, to enhance the chiral induction efficiency in CLC materials, it is essential to optimize oligomer length to achieve better compatibility, as seen through the lens of dichroism and polymer compatibility.

Then we explored deeper into the CPL performance by evaluating four emissive CLCs within flat cells. The fluorescence quantum yield of CLCs were measured to be 80%, 74%, 70% and 35%, respectively. Remarkably, each CLC demonstrated robust and distinct CPL signals at 500 nm and 550 nm, mirroring the FL emission spectra of achiral dyes, as shown in Fig. 5b, Figs. S7 and S8 (Supporting information). Crucially, the magnitude of the CPL ($|g_{lum}|$) for the CLCs reflected the trends seen in the CD intensities presented in Fig. 5a. For the CLC with the smallest spontaneous polarization (S_F) of 0.20 (CLCs-M1), the $|g_{lum}|$ was a mere 0.35, correlating with its weak CD signal and the lower degree of order ($S_F = 0.20$) within the LC host. As S_F values increased, the $|g_{lum}|$ for CLCs-M2 and CLCs-M3 rose significantly, reaching 0.71 and 0.84 respectively. The pronounced enhancement for M3 ($|g_{lum}| = 0.84$) is likely due to the efficient transfer of chirality from the chiral dopant to the achiral dichroic M3, resulting in a helical structure within the well-ordered CLC matrix [51]. In the case of F8BT, the $|g_{lum}|$ values echoed the CD spectral trend, with compatibility markedly influencing CPL intensity. This suggests that compatibility and the large aspect ratio of the conjugated polymer are critical factors affecting the CPL intensity in emissive CLC materials. Achieving a balance between dichroism and compatibility is crucial for optimizing CPL in conjugated polymer-doped CLCs.

In summary, our research explored the impact of conjugation length on CLC systems through the integration of oligomers M1-M3 and the polymer F8BT into a CLC matrix. Among these, oligomer M3 exhibited the most significant increase in g_{lum} value, achieving an optimal balance between its dichroic properties and compatibility with the host CLC. We observed that an increase in the conjugation length of the conjugated polymers tends to enhance dichroism, attributed to a larger length-to-diameter ratio. However, this often leads to reduced compatibility, especially as the polymers become less congruent with the CLC host structure. Therefore, oligomeric conjugated polymers emerge as prime candidates for CLC-based, CPL-active systems, thanks to their exceptional photophysical characteristics and high compatibility. By employing a chiral co-assembly approach, our study provides a simple method for the regulation of CPL signals and lays down fundamental scientific principles for the design of CLC-based CPL materials.

Declaration of competing interest

The authors declare that they have no known competing financial interests or personal relationships that could have appeared to influence the work reported in this paper.

CRediT authorship contribution statement

Yang Li: Conceptualization, Writing – original draft, Writing – review & editing. **Yihan Chen:** Data curation, Investigation. **Jiaxin Luo:** Formal analysis, Methodology. **Qihuan Li:** Formal analysis, Methodology. **Yiwu Quan:** Supervision, Validation. **Yixiang Cheng:** Funding acquisition, Supervision, Writing – review & editing.

Acknowledgment

This work was supported by the National Natural Science Foundation of China (Nos. 21975118, 92156014, 52373188).

Supplementary materials

Supplementary material associated with this article can be found, in the online version, at doi:10.1016/j.cclet.2024.109864.

References

[1] H.K. Bisoyi, Q. Li, Chem. Rev. 122 (2022) 4887–4926.
[2] K. Akagi, Chem. Rev. 109 (2009) 5354–5401.
[3] L. Wan, Y. Liu, M.J. Fuchter, B. Yan, Nat. Photonics 17 (2023) 193–199.
[4] M. Chapran, E. Angioni, N.J. Findlay, et al., ACS Appl. Mater. Interfaces 9 (2017) 4750–4757.
[5] H. Yu, B. Zhao, J. Guo, K. Pan, J. Deng, J. Mater. Chem. C 8 (2020) 1459–1465.
[6] S.Y. Lin, H. Sun, J.H. Qiao, X.K. Ding, J.B. Guo, Adv. Opt. Mater. 8 (2020) 2000107.
[7] S. Lin, Y. Tang, W. Kang, et al., Nat. Commun. 14 (2023) 3005.
[8] P. Fan, Z. Fang, S. Wang, et al., Chin. Chem. Lett. 34 (2023) 107934.
[9] D.J. Mulder, A.P.H.J. Schenning, C.W.M. Bastiaansen, J. Mater. Chem. C 2 (2014) 6695–6705.
[10] Y.K. Kim, X. Wang, P. Mondkar, E. Bukusoglu, N.L. Abbott, Nature 557 (2018) 539–544.
[11] Y. Wu, C. Yan, X.S. Li, et al., Angew. Chem. Int. Ed. 60 (2021) 24549–24557.
[12] M. Li, H. Hu, B. Liu, et al., J. Am. Chem. Soc. 144 (2022) 20773–20784.
[13] Q. Guo, M. Zhang, Z. Tong, et al., J. Am. Chem. Soc. 145 (2023) 4246–4253.
[14] S. Jiang, S. Zhou, Y. Chen, H. Guo, F. Yang, Chin. Chem. Lett. 33 (2022) 2442–2446.
[15] G. Zhang, X. Cheng, Y. Wang, W. Zhang, Aggregate 4 (2023) e262.
[16] J. Wade, J.R. Brandt, D. Reger, et al., Angew. Chem. Int. Ed. 60 (2021) 222–227.
[17] Y. Shi, J. Han, X. Jin, et al., Adv. Sci. 9 (2022) 2201565.
[18] J.L. Yan, F. Ota, B.A. San Jose, K. Akagi, Adv. Funct. Mater. 27 (2017) 1604529.
[19] D.Y. Zhao, H.X. He, X.G. Gu, et al., Adv. Opt. Mater. 4 (2016) 534–539.
[20] Y. Chen, P. Lu, Z. Li, et al., ACS Appl. Mater. Interfaces 12 (2020) 56604–56614.
[21] W. Gong, G. Huang, M. Zhou, et al., ACS Appl. Mater. Interfaces 15 (2023) 49701–49711.
[22] K. Yao, Y. Shen, Y. Li, et al., J. Phys. Chem. Lett. 12 (2021) 598–603.
[23] Y. Li, Y. Shen, K. Liu, Y. Quan, Y. Cheng, Dyes Pigm. 186 (2021) 109001.
[24] X. Li, W. Hu, Y. Wang, Y. Quan, Y. Cheng, Chem. Commun. 55 (2019) 5179–5182.
[25] Y. Bao, G. Zhang, N. Wang, M. Pan, W. Zhang, J. Mater. Chem. C 11 (2023) 2475–2479.
[26] Q. He, T.L. Dexter Tam, T. Lin, et al., ACS Macro Lett. 11 (2022) 1136–1141.
[27] C. Kulkarni, R.H.N. Curvers, G. Vantomme, et al., Adv. Mater. 33 (2020) e2005720.
[28] G. Zhang, Y. Bao, M. Pan, et al., Sci. China Chem. 66 (2023) 1169–1178.
[29] Y. Chen, Z. Xu, W. Hu, et al., Macromol. Rapid Commun. 42 (2021) 2000548.
[30] D. Xu, X. Hua, C. Liu, et al., ACS Appl. Mater. Interfaces 15 (2023) 25783–25790.
[31] Y. Chen, Y. Zhang, H. Li, et al., Adv. Mater. 34 (2022) 2202309.
[32] Y. Li, Y. Chen, H. Li, et al., Angew. Chem. Int. Ed. 62 (2023) e202312159.
[33] K.P. Fritz, G.D. Scholes, J. Phys. Chem. B 107 (2003) 10141–10147.
[34] A. Abdulkarim, F. Hinkel, D. Jänsch, et al., J. Am. Chem. Soc. 138 (2016) 16208–16211.
[35] M. Mamada, R. Komatsu, C. Adachi, ACS Appl. Mater. Interfaces 12 (2020) 28383–28391.
[36] L. Pu, Chem. Rev. 98 (1998) 2405–2494.
[37] Y. Li, K. Yao, Y. Chen, Y. Quan, Y. Cheng, Adv. Opt. Mater. 9 (2021) 2100961.
[38] R. Liu, G. Zhu, Y. Ji, G. Zhang, Eur. J. Org. Chem. 2019 (2019) 3217–3223.
[39] M.G. Debije, C. Menelaou, L.M. Herz, A.P.H.J. Schenning, Adv. Opt. Mater. 2 (2014) 687–693.
[40] X. Zhang, H. Gorohmaru, M. Kadowaki, et al., J. Mater. Chem. 14 (2004) 1901–1904.
[41] A.M. Kendhale, A.P.H.J. Schenning, M.G. Debije, J. Mater. Chem. A 1 (2013) 229–232.
[42] M.T. Sims, L.C. Abbott, S.J. Cowling, J.W. Goodby, J.N. Moore, Phys. Chem. Chem. Phys. 19 (2017) 813–827.
[43] M.T. Sims, R.J. Mandle, J.W. Goodby, J.N. Moore, Liq. Cryst. 44 (2017) 2029–2045.
[44] J. Sol, V. Dehm, R. Hecht, et al., Angew. Chem. Int. Ed. 57 (2018) 1030–1033.

[45] Y. He, S. Zhang, H.K. Bisoyi, et al., Angew. Chem. Int. Ed. 60 (2021) 27158–27163.
[46] Y. He, Q. Fan, J. Gao, H. Chen, J. Guo, Mater. Chem. Front. 6 (2022) 1844–1849.
[47] K. Yao, Y. Li, Y. Shen, Y. Quan, Y. Cheng, J. Mater. Chem. C 9 (2021) 12590–12595.
[48] K. Yao, Z. Liu, H. Li, et al., Sci. China Chem. 65 (2022) 1945–1952.
[49] Y. Xia, A. Hao, P. Xing, Chin. Chem. Lett. 33 (2022) 4918–4923.
[50] L. Ji, Y. Zhao, M. Tao, et al., ACS Nano 14 (2020) 2373–2384.
[51] Y. Chen, Y. Li, H. Li, et al., Sci. China Chem. (2023), doi:10.1007/s11426-023-1846-0.